

MAPPING TECHNIQUES FOR MONTE CARLO MODELLING OF THE ELECTRON DISTRIBUTION FUNCTION IN A STELLARATOR*

Sergei V. Kasilov¹, Winfried Kernbichler², Viktor V. Nemov¹, and **Martin F. Heyn**²

¹*Institute of Plasma Physics, National Science Center “Kharkov Institute of Physics and Technology”, Ul. Akademicheskaya 1, 310108 Kharkov, Ukraine*

²*Institut für Theoretische Physik, Technische Universität Graz, Petersgasse 16, A-8010 Graz, Austria*

1. Introduction

When studying various physical aspects of fusion devices, a detailed knowledge of the particle distribution functions in coordinate space as well as in velocity space is required. Such problems can be the determination of power deposition profiles in particular fusion devices during electron cyclotron resonance heating (ECRH), the creation of currents favourable or unfavourable for plasma confinement, in diagnostics the interpretation of electron cyclotron emission lines in presence of suprathermal electron populations, the theoretical description of the creation of unstable distributions during ECRH in stellarator devices [1], and others.

The governing equation to be solved is the 5D drift kinetic equation. Regular methods, i.e., all methods not based on stochastic steps, can only be applied if sufficient symmetries exist which can be used to reduce the dimensionality of the problem. Stochastic methods like Monte Carlo (MC) are therefore preferable if a reduction of dimensionality is not possible [2]. MC methods are simply to apply but in order to obtain a good resolution, millions of stochastic trajectories have to be followed. Even on present-day fast parallel computers time becomes a severe constraint.

On the other hand, in circumstances where τ_c the typical collision time is large compared to τ_b the typical bounce time in a toroidal or ripple magnetic well, a tremendous amount of computer time is wasted in re-computing again and again the drift orbits which are only slightly perturbed by collisions. To overcome the numerical stiffness in these time scales, a stochastic mapping technique had been developed [3]. First results from such a stochastic mapping code for stellarator geometry are presented.

2. Stochastic Mapping

The drift kinetic equation in general coordinates $z = (\vartheta, \mathbf{u}) \equiv (\vartheta, x^1, x^2, p, \lambda, t)$, with ϑ , x^1 , x^2 generalised space coordinates, λ the pitch angle cosine, p the momentum module, and t the time, is

$$V^i \frac{\partial f}{\partial z^i} = \frac{1}{J} \frac{\partial}{\partial z^i} J \left(D^{ij} \frac{\partial f}{\partial z^j} - F^i f \right) - \nu_0 f + Q, \quad i, j : (\vartheta, \mathbf{u}), \quad (1)$$

where the lhs describes convection along the guiding centre drift orbit and the rhs collisions and quasilinear effects. In the limit of rare collisions, the variation of the distribution function on drift orbits is of first order in τ_b/τ_c and the rhs can be treated as a perturbation. Poincaré cuts (4D hypersurfaces) in phase space are introduced in a convenient way, e.g., minimum

*This work was partly supported by the Association EURATOM-OEAW under contract number ERB 5004 CT 96 0020 and by the Ukrainian Foundation of Fundamental Research project 2.4/699.

B surfaces. Using the low collisionality assumption and integrating the equation along the collisional unperturbed drift orbits between their intersection points with subsequent cuts, a set of second kind Fredholm integral equations is obtained [3] which relates the fluxes per unit area $\Gamma_m(\mathbf{u})$ at the intersection points through the relevant Poincaré cuts defined by $\vartheta = \vartheta_m(\mathbf{u})$,

$$\begin{aligned} \Gamma_{m'}(\mathbf{u}') &= \sum_m \int d^5u \delta_{m',M_m(\mathbf{u})} \delta(\mathbf{u}' - \mathbf{U}_m(\mathbf{u})) \\ &\times \left\{ \int d^5u'' \left[[1 - \bar{\nu}_{0m}(\mathbf{u}'')] \delta(\mathbf{u} - \mathbf{u}'') \right. \right. \\ &+ \left. \left. \bar{D}_m^{ij}(\mathbf{u}'') \frac{\partial^2 \delta(\mathbf{u} - \mathbf{u}'')}{\partial u^i \partial u^j} - \mathcal{F}_m^i(\mathbf{u}'') \frac{\partial \delta(\mathbf{u} - \mathbf{u}'')}{\partial u^i} \right] \Gamma_m(u'') \right. \\ &\left. + \mathcal{Q}_m(\mathbf{u}) \right\}. \end{aligned} \quad (2)$$

The essential point is that the integral kernel of (2) consists of two separate parts; a deterministic operator based solely on the drift orbit dynamics $\mathbf{U}_m(\mathbf{u})$, and a stochastic operator based on orbit integrated diffusion coefficients, sinks, and sources, $\bar{D}_m^{ij}(\mathbf{u})$, $\mathcal{F}_m^i(\mathbf{u})$, $\bar{\nu}_{0m}(\mathbf{u})$, and $\mathcal{Q}_m(\mathbf{u})$.

In a preloading phase, the drift dynamics as well as the orbit integrated quantities are computed and the results are stored for each cut separately. Instead of performing a ‘tiny’ step along the drift orbit followed by a stochastic step consistent with D^{ij} and F^i as it is done in direct MC codes, stochastic mapping performs a ‘huge’ step along the drift orbit, i.e., a map, followed by a stochastic step consistent with $\bar{D}_m^{ij}(\mathbf{u})$ and $\mathcal{F}_m^i(\mathbf{u})$. For typical fusion configurations with a simple magnetic field model, the gain in speed of stochastic mapping as compared with direct MC turns out to be a factor of 100 and is expected to be even 1 or 2 orders of magnitude higher for more realistic magnetic field models.

3. Results

Stochastic mapping has been implemented into a code designed for stellarator geometry of at most one magnetic field minimum per magnetic field period, e.g., $2\pi/9$ for URAGAN-3M L=3 torsatron. The drift orbits, respectively their intersection points with the cuts, obtained by mapping as well as the radial diffusion coefficient obtained by stochastic mapping have been tested against the drift orbits obtained by direct Runge-Kutta integration and the radial diffusion coefficient obtained by direct MC. All comparisons show good agreement and with this confidence the more complex problem of computing the stationary Green’s function is addressed. Such type of Green’s functions have been successfully used to study localised electron cyclotron heating in stellarators [4]. In this case, the collision operator in (1) represents Coulomb collisions of test particles with an isotropic Maxwellian background plasma. Particles with 9 times the thermal energy and different pitch angles are injected on a specific magnetic surface into a background plasma with $n = 10^{13} \text{ cm}^{-3}$, $T = 1 \text{ keV}$, and $B = 10 \text{ kG}$. The stochastic particle trajectory is followed until it leaves the confinement volume or until the particle becomes thermalized.

The results for ripple trapped injected electrons are shown in Figures 1 and 2. Such particles do not experience the rotational transform and therefore they are subject to considerable drift motions towards the boundaries of the confinement volume (downwards for the present configuration). Figure 1c shows the electron distribution as it would be seen on the minimum B cut. It can be observed how collisional transport populates the neighbouring magnetic surfaces

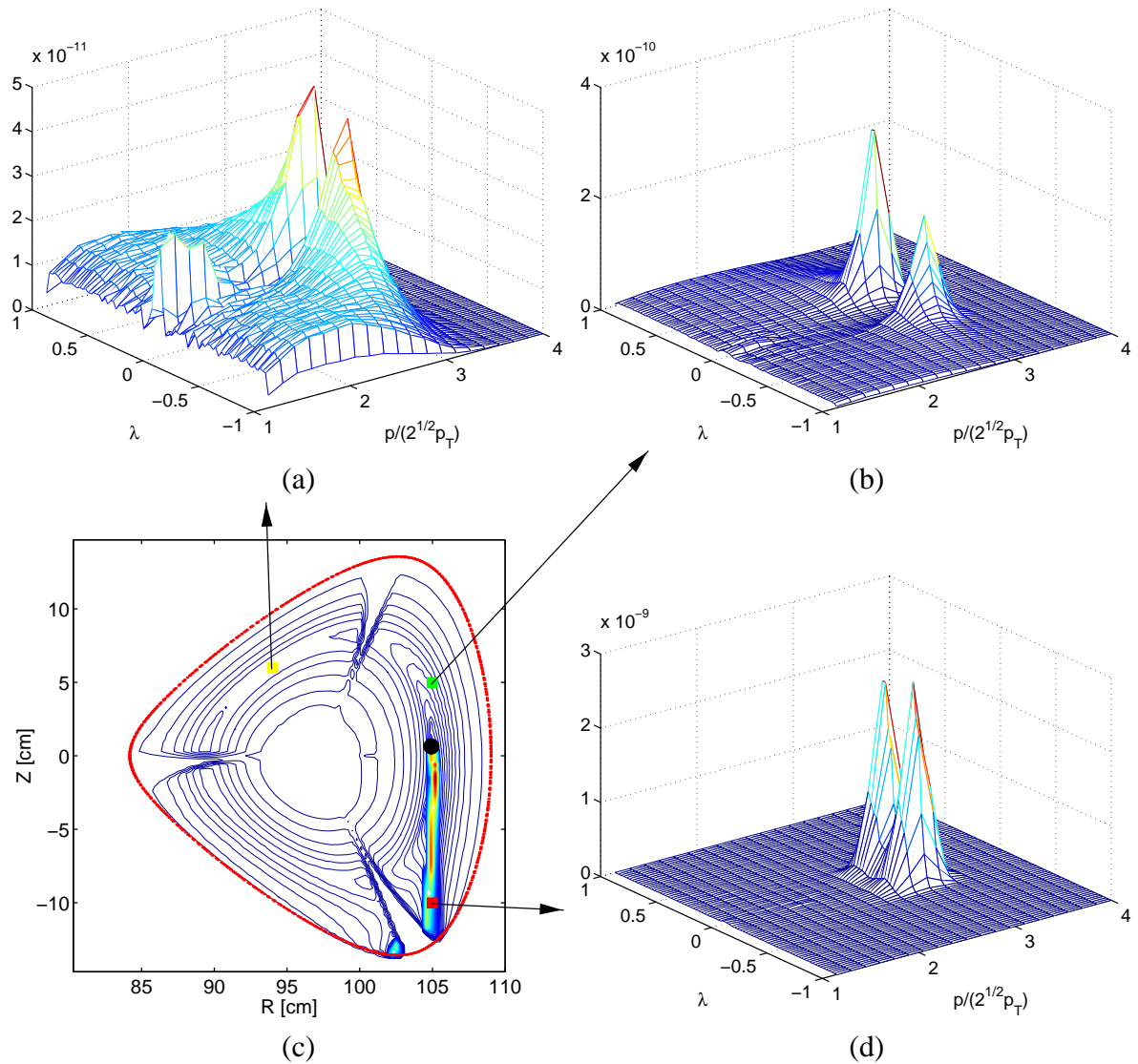


Figure 1. (c) contours of the electron density on the minimum-B cut projected along magnetic field lines onto the reference cut $\varphi = 0$. For the space points marked in (c), the detailed velocity space distributions are shown in (a), (b), and (d), respectively. The source point of electron injection (solid circle) in phase space is $R = 105$ cm, $Z = 1$ cm, $\lambda = 0.15$, and corresponds to ripple trapped particles.

with electrons. Also shown in the figure are the distributions of electrons in velocity space for the 3 different locations indicated in (c). The distribution (d) shows the primary fate of the electrons injected, i.e., ripple trapped particles drifting downwards not having had enough time to thermalize substantially. The two spikes correspond to co- and counter streaming ($\lambda \neq 0$) electrons which are slightly thermalized. The electron velocity distribution (a) for a distant point on the same magnetic surface the particles are injected from, shows a two orders of magnitude smaller population of banana-like and passing electrons and the also abundance of ripple trapped particles as expected. Finally, the asymmetry of the magnetic ripple wells leads to an asymmetric detrapping and eventually re-trapping of electrons as can be seen in (b) for a point nearby the injection point.

Figure 2 shows the corresponding current density distribution in the device. The originally ripple trapped electrons produce practically no current but, as a result of collisions, also

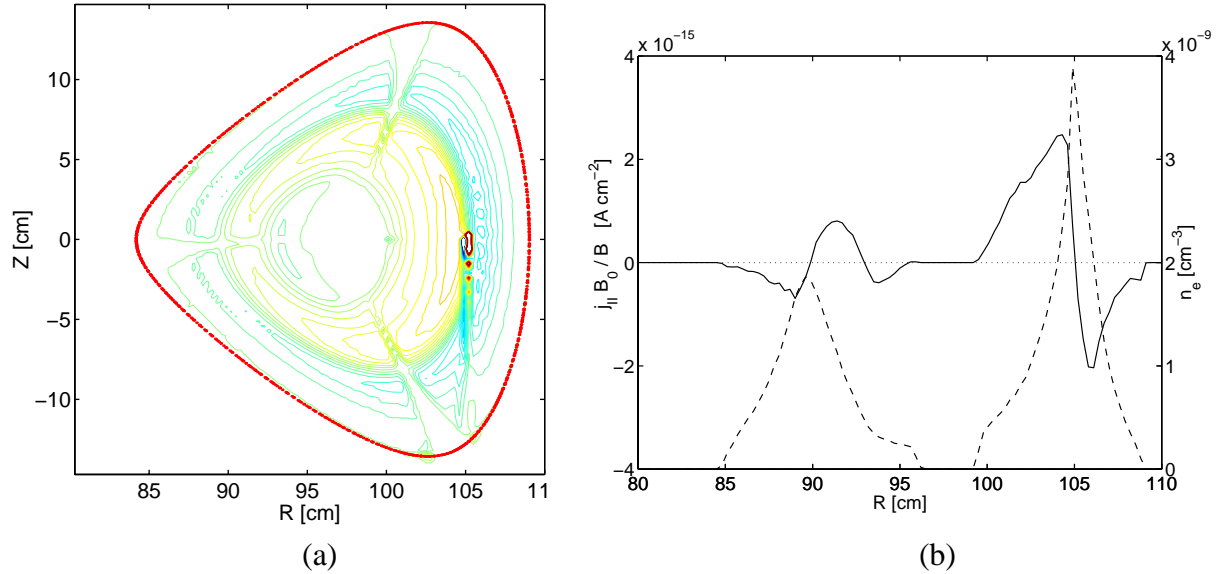


Figure 2. (a) contours of $j_{\parallel} B_0 / B$ the parallel current density through the minimum-B cut normalised to the magnetic field module. (b) electron density (dashed) and normalised parallel current density (solid) as functions of the big radius R for $Z = 1.5$ cm.

passing and toroidally trapped banana type electrons occur. The distribution of detrapped electrons is asymmetric in general and parallel currents will appear. A significant fraction of the current is due to finite width banana electrons non-uniformly distributed with respect to the radius (bootstrap-like effect). The electron density and current density profiles displayed in Figure 2b demonstrate that the bipolar current is uniquely related to the electron density gradient.

4. Summary

In the present contribution, the first results of the implementation of the stochastic mapping technique into a code for stellarator geometry are presented and discussed. The results have been checked against results from direct MC calculations and have been shown to agree within the limits of validity of stochastic mapping ($\tau_b \ll \tau_c$). At the same time, the gain in speed of stochastic mapping as compared with direct MC is found to be several orders of magnitude and depends to a large extent on the magnetic field model. This allows one to compute particle distribution functions in the full 5D phase space of the drift kinetic equation. The high computational speed of the stochastic mapping code guarantees a good resolution of the distribution function obtained. This has been demonstrated by modelling the Green's function used to study localised ECRH. The result shows the appearance of complicated induced current profiles in stellarators generated by localised ECRH.

References

- [1] Romé, M., Erckmann, V., Gasparino, U., Hartfuß, H.J., Kühner, G., Maaßberg, H., and Marushchenko, N., *Plasma Phys. Contr. Fusion*, **39**, 117–158 (1997)
- [2] Murakami, S., Okamoto, M., Nakajima, N., Ohnishi, M., and Okada, H., *Nucl. Fusion*, **34**, 913–925 (1994)
- [3] Kasilov, S.V., Moiseenko, V.E., and Heyn, M.F., *Phys. Plasmas*, **4**, 2422–2435 (1997)
- [4] Murakami, S., Gasparino, U., Maaßberg, H., Marushchenko, N., Nakajima, N., Okamoto, M., and Romé, M., *J. Plasma Phys. and Fusion Res.*, **1**, 122–125 (1998)